arXiv:cond-mat/0611604v1 [cond-mat.mes-hall] 23 Nov 2006

Graphene Switch Design: an Illustration of the Klein Paradox

Q. W. Shi,[1] Z. F. Wang,[1] Jie Chen,[2] Huaixiu Zheng,[2] Qunxiang Li,[1] Xiaoping Wang,[1] Jinlong Yang,[1,*] and J. G. Hou[1]

[1] *Hefei National Laboratory for Physical Sciences at Microscale, University of Science and Technology of China, Hefei, Anhui 230026, People's Republic of China*

[2] *Electrical and Computer Engineering, University of Alberta, AB T6G 2V4, Canada*

An armchair graphene ribbon switch has been designed based on the principle of the Klein paradox. The resulting switch displays an excellent on-off ratio performance. Anomalous tunneling phenomena are observed in our numerical simulations. According to our analytical results, selective tunneling rule is proposed to explain this interesting transport behavior. The switch design enriches the phenomenon of the Klein paradox and also provides a platform to study the paradox.

PACS numbers: 85.65.+h, 73.63.-b,73.61.Wp

The recent fabrication of graphene has attracted a lot of research interest.[1,2,3,4,5,6] Graphene consists of a single atomic layer of graphite, which can also be seen as a sheet of an unrolled carbon nanotube. The edge carbon atoms of graphene ribbons have two typical topological shapes: namely armchair and zigzag. Zigzag graphene ribbon has a localized state near the Fermi level, which originates from a gauge field produced by lattice deformation.[7] Such a localized state, however, does not appear in armchair graphene ribbons. Armchair graphene ribbon can be easily made to be either metallic or semiconducting by controlling its width.[8] This remarkable characteristic is very attractive in making graphene-based nanoscale devices. Moreover, a graphene ribbon is easier to manipulate than carbon nanotube (CNT) due to its flat structure, and thus it can be tailored by using conventional lithography techniques. The minimal conductivity resulting from its infinite two-dimensional (2-D) graphene structure and its gap-less energy band structure, however, limits the performance of the 2-D graphene devices due to its poor on-off ratio.[9] Semiconducting graphene ribbon is expected to resolve this on-off ratio problem.

Very recently, Geim's group proposed an experimental realization of prediction of the so-called Klein paradox in a 2-D graphene system.[9] The Klein paradox predicts that the electron can pass through a high potential barrier without exponential decay.[10] In this letter, we design a graphene ribbon switch by utilizing such a paradox and study the associated tunneling problem in a quasi-one-dimensional system. For this purpose, we consider a semiconducting armchair junction connecting to a left and a right metallic armchair graphene leads. Due to the band gap in our junction, the electron within the energy gap is prohibited to transmit through the junction without applied gate voltage, and the graphene switch stays in the 'off' state. The junction can be turned 'on' when an external gate voltage exceeds a threshold voltage. In addition to the good on-off ratio performance of the proposed switch, our design also provides a platform upon which to confirm the Klein paradox. Unlike the 2-D graphene system, in which electrons have to conserve their chirality in order to pass through the barrier, in the quasi-1D graphene system, due to the confined boundary, certain selective tunneling should be satisfied for the resonant transmission of electrons.

Our setup is shown in Fig. 1, in which a semiconducting armchair graphene is connected to two metallic semi-infinite armchair graphene ribbon leads. The bottom subgraph of Fig. 1 shows the atomic structure of the graphene junction including three regions: left lead, middle graphene region, and right lead. Both leads have the same width with $W = 3m - 1$ to ensure that they are metallic. The width of the middle region is chosen to be $W + 4$ so that it is semiconducting.[8] The top subgraph in Fig. 1 shows the dispersion relation of the left, middle and the right region of the switch, respectively. The dashed line denotes the energy E of incident electrons. U is the external potential applied to the middle graphene region. Unlike conventional parabolic semiconductor energy band diagram ($\mathbf{E} \propto \mathbf{k}^2$), the energy of the lowest conduction subband in the lead is linearly proportional to vector $\mathbf{k}$.[2] This dispersion relation indicates that carriers in this channel are massless.

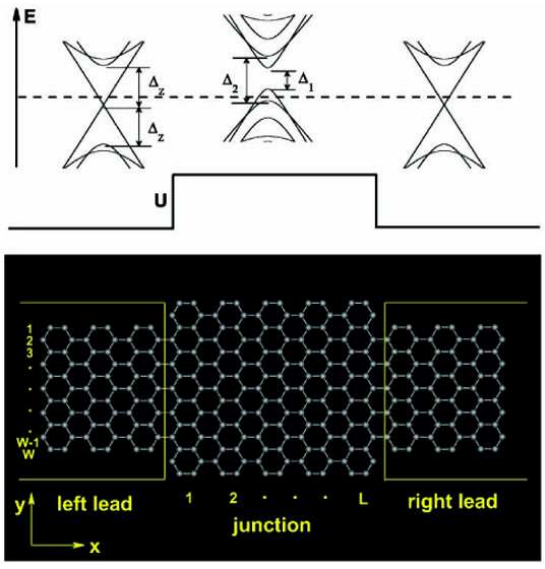


FIG. 1: (color online) Schematic diagrams of the energy band dispersions and the proposed graphene switch.

The conductance G of the switch is calculated by using the Landauer-Büttiker formula ($G=\frac{2e^2}{h}T$).[11] The transmission function T is obtained by the recursive Green's function method.[12,13] In order to ensure the incident electron energy lies within the single-mode region of the leads and also in the gap of the middle graphene region, we choose $E<\min(\frac{\Delta_1}{2}, \Delta_z)$. As shown in Fig. 1, Δ_1 is the band gap between the lowest conduction subband and the upmost valence subband of the junction, Δ_z is the energy spacing between the bottom of conduction subbands and the next subband within the lead. In the following simulations, we set W=23 and thus obtain the corresponding Δ_z=0.65 eV, Δ_1=0.38 eV and Δ_2=0.79 eV by the nearest neighbor tight-binding band structure calculation.[14] The calculated conductances are shown in Fig. 2. By applying an external gate voltage at the middle graphene region, a potential barrier U appears. In general, if the chosen voltage potential makes the energy of incident electron touch the first top of the valence subband of the junction, the incident electron can easily pass through the junction as expected and the switch should be turned 'on'. However, our simulating result shows that the incident electrons are almost reflected completely and the conductance remains almost zero. This phenomenon implies that the carrier has to satisfy an additional condition to pass through the potential barrier.

When the potential barrier U increases further, the switch turns 'on' and the first resonant transmission peak appears around U=0.51 eV for L=20. This behavior can be easily understood by the Klein's paradox. That is, with the help of the hole's channels, the electrons can transfer through the large potential barrier without exponential decay. The conductance oscillates above the envelope line and increases as U increases due to the resonance and antiresonance transports, as shown in Fig. 2. As the length of the junction increases, the first resonant peak becomes sharper and shifts towards left slightly and more resonant peaks appear. These observations are easily understood by the conventional resonance condition. However, to produce the first conductance peak, the condition $U> \Delta_2/2+E$=0.44 eV is still required. This result strongly suggests that this peak results from the second valence subband.

Fig. 3 shows the conductance as a function of the junction length L calculated by fixing E=0.05 eV and U=0.5 eV. Such a choice provides two conducting channels in the middle region for electrons passing through the junction. In general, the conductance curve should be complicated with some glitches due to the quantum interference between two channels.[13] Surprisingly, our numerical result exhibits a regular periodicity as a function of L in Fig. 3. Based on the detailed analysis of this conductance period with the conventional resonance condition, we find that only the second valence subband provides a channel to allow incident electrons pass, and the first valence subband does not contribute. To verify this finding, similar simulations were performed by changing the width of graphene ribbon junction to $W = 17$ and $W = 20$ and the same phenomenon was observed.

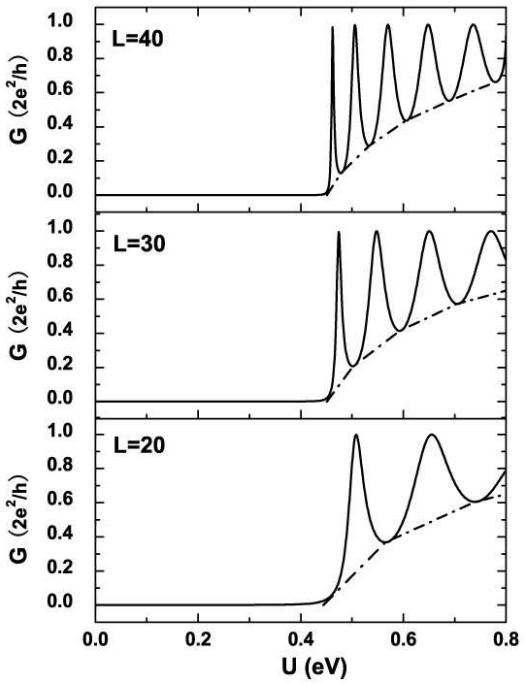


FIG. 2: Conductance vs. the potential height in the single-mode region with different length of the junction. Here W = 23 and $E = 0.05eV$. The conductance oscillates above the envelope line plotted with dash dot line.

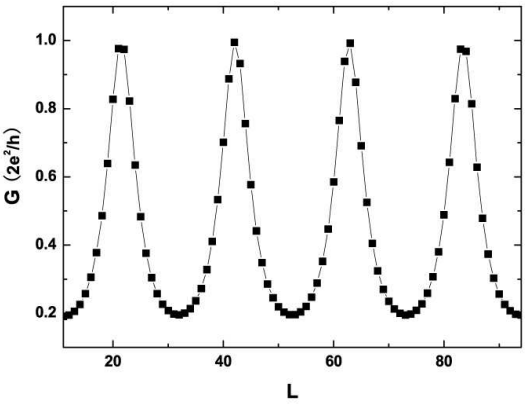


FIG. 3: Conductance versus the length of the junction with $W = 23$, $E = 0.05eV$ and $U = 0.5eV$.

Generally speaking, to pass through the middle region, electrons have to satisfy conventional resonance condition which usually describes the transfer of an electron through a junction via resonant tunneling (T=1) due to the phase accumulation. It works well in conventional semiconductor when the Schröedinger equation is used. In our switch model, the valence subbands in the conductor can be shifted upwards with the applied external gate voltage and provides conducting channels. When electrons satisfy the convention resonance condition, q_xL=Nπ with N=0,±1,±2,..., here, q_x denotes the

x-direction (along the propagation direction) component of wave-vector inside the middle region, they can pass through the junction resonantly. However, our simulation results show that the electron is still prohibited to pass trough the middle region when the conventional resonance condition is satisfied. To understand this anomalous transport behavior more clearly, we derive an analytical expression of the eigenfunction and eigenvalue of the perfect armchair graphene ribbon with a finite width (W) as

$$\psi_n^s(j,q_x) = \frac{sin(q_n\frac{\sqrt{3}}{2}aj)}{\sqrt{(W+1)\frac{\sqrt{3}}{2}a}} \begin{pmatrix} 1 \\ s\sqrt{\frac{\mu^*}{\mu}} \end{pmatrix} \quad (1)$$

$$\varepsilon_n^s(q_x) = sV\sqrt{\mu\mu^*} \quad (2)$$

with μ=$2e^{iq_x\frac{a}{2}}cos(q_n\frac{\sqrt{3}}{2}a) + e^{-iq_x a}$, $q_n = \frac{n\pi}{\frac{\sqrt{3}}{2}a(W+1)}$, respectively. Here, a is the C-C bond length (1.42Å), V is the nearest hopping parameter (-3.0 eV), n denotes different subband with 1, $\cdots$, W, j labels the atomic position in the y-direction with 1,$\cdots$,W, and s=1 and -1 describes the conduction subbands and the valence subbands, respectively. The chirality of the electron in the conduction subband or hole in the valence subband can be determined by the good quantum number q_x and q_n. To determine the lowest conduction subband or the upmost valence subband, the integer number n needs to satisfy the condition n=$Nint[\frac{2}{3}(W+1)]$. Here the function of *Nint* rounds off the variable to a integer. To verify that electrons in the lowest conduction subband cannot pass through the switch, we calculate the corresponding transfer matrix element P_{11}, and we obtain P_{11}=$|\langle s,n,q_x|\hat{V}|s',n',q_x'\rangle|^2 \simeq 4.5\times10^{-14}$ eV^2 with s=+1, n=16, s'=-1, and n'=19. Here, $\hat{V}$=$V\sum_j |j\rangle\langle j+2|$ with j=2,4,6, $\cdots$,W-1 is the scattering operator coming from the sharp interface between the lead and the middle region. In the elastic scattering process in our system, the equation $\varepsilon_n^{+1}(q_x)$=$\varepsilon_{n'}^{-1}(q_x')+U$ has to be satisfied. Meanwhile, the applied voltage U is large enough to ensure the equation have a real numerical solution (q_x'). The transfer matrix element P_{12} between the lowest conduction subband to the second upmost valence subband is calculated to be around 0.27 eV^2. In our switch the value of these transfer matrix elements are almost independent of the width of graphene ribbon based on our numerical simulations.

Unlike its 2-D counterpart,[10] the sharp interface in our design plays an important role. From our numerical results, it is clear that the selective tunneling corresponding to two transfer matrix elements (P_{11} and P_{12}) can illustrate the interesting transport process. When U>0.24 eV, the first valence subband of the middle graphene junction is moved high enough to provide a conducting channel, but P_{11} almost equals to zero. That is to say, no matter whether the chirality of electrons conserves or not, the sharp interface in this symmetrical connection prevents tunneling process. Electrons, therefore, are bounced back and the conductance remains almost zero, as shown in Fig. 2. Increasing the length of the junction only changes the conventional resonance condition, but the conductance still remains zero. When we further increase the voltage potential to U>0.44 eV, the second valence subband of the middle junction moves upwards. The energy of incident electrons touches this channel and the electrons can then tunnel through the potential barrier without exponential decay.

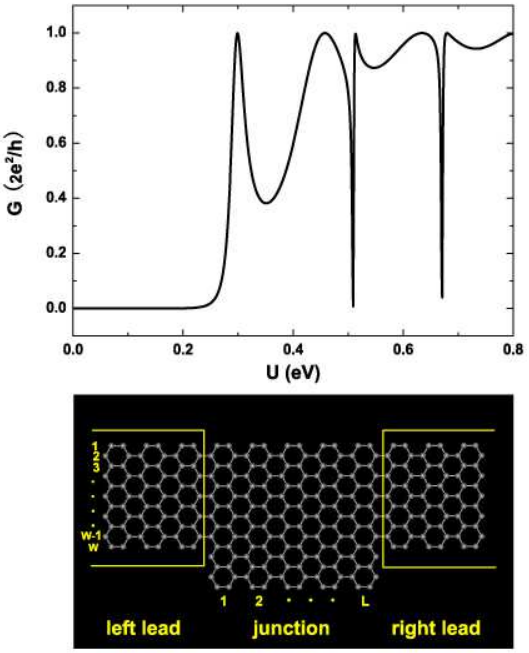


FIG. 4: (color online) Top subgraph: conductance vs. the potential height in the single-mode region. Bottom subgraph: atomic structure of the T-shaped junction. Here W = 23, L = 20 and E = 0.05eV.

It should be pointed out that whether the first valence subband contributes to the conductance or not depends strongly on the geometric structure of the graphene ribbon junction. As an example, a T-shaped junction with the same width of the previous symmetry structure is shown in Fig. 4. By choosing the same parameters (E=0.05 eV, W=23 and L=20) as in the case of Fig. 3, numerical results in Fig. 4 show clearly that the first conductance peak appears in the region where the incident energy touches the first valence subband (0.24 eV<U<0.44 eV). The reason is that the transfer matrix element (P_{11}) has a finite value (about 0.24 eV^2) in T-shaped junction. Our results suggest that the switch conducting behavior can be manipulated by tailoring the graphene ribbon. In the range of 0.44 eV<U<0.7 eV, another interesting observation is that two obvious conductance dips appear in the conductance curve. This phenomenon can be attributed to the destructive interference effect between two conducting channels.[15]

To illustrate the switch effect more clearly in the single-mode region, Fig. 5 presents a three-dimensional color

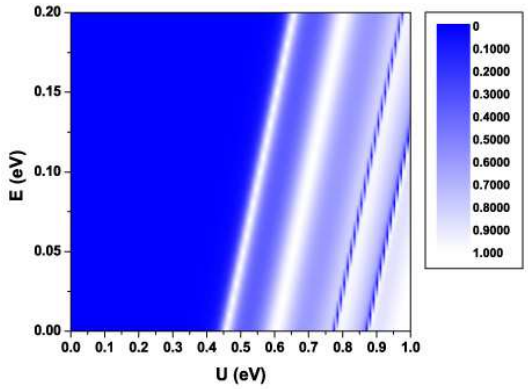


FIG. 5: (color online) Three-dimensional plot of conductance as the function of energy and potential height for the configuration shown in Fig.1. Here $W = 23$ and $L = 20$.

picture to display the conductance as a function of incident electron energy (E) and the potential barrier height (U) for the configuration shown in Fig.1. The color is scaled with the corresponding conductance, white and blue colors correspond to T=1 ('on') and T=0 ('off'), respectively. It is clear that the figure can be roughly divided into two regions bounded by the first peak (the most left white line). At the left of the first peak (the first white line), the switch stays shut off or all incident electrons are bounced back. The junction begins to be turned 'on' starting from the right of the first peak by applying a certain threshold bias U and its conductance oscillates with increasing U as shown in Fig. 2. Although more channels can allow electrons pass through or more resonance matching conditions can be satisfied as U increases, T never exceed '1'. The reason is that the energy of incident electron is limited within the single-mode region in our calculations. Several additional interesting features can be observed in Fig. 5: (i) the peaks or the white lines are parallel to each other and shift toward the right as the incident energy increases. (ii) all peaks are straight lines indicating the required voltage to open the switch increases linearly as incident electron energy increases. (iii) the white lines become wider and blue lines become narrower as U increases.

In conclusion, the transport properties of a semiconducting graphene ribbon sandwiched between two metallic graphene ribbon leads are investigated. Switching behavior is observed according to our numerical results. The junction has a good on-off ratio performance, which is almost completely pinched-off without external gate voltage and can be turned 'on' by applying a threshold bias voltage. We find that our numerical results are related closely to the Klein phenomenon. Electron can pass through the junction when these Dirac Fermions satisfy both the conventional resonance condition and the selective tunneling rule. These findings are helpful for us to construct and design graphene nanoelectronic devices in the near future.

The authors would like to thank Michael Brett for his discussions and support. We also would like to thank Shawn Sederberg and Woon Tiong Ang for their assistance with the finalization of this paper. This work is partially supported by the National Natural Science Foundation of China, by National Key Basic Research Program under Grant No. 2006CB0L1200, by the USTC-HP HPC project, and by the SCCAS and Shanghai Supercomputer Center. Jie Chen would like to acknowledge the funding support from the Discovery program of Natural Sciences and Engineering Research Council of Canada (No. 245680).

* Corresponding author. E-mail: jlyang@ustc.edu.cn

[1] K. S. Novoselov, A. K. Geim, S. V. Morozov, D. Jiang, Y. Zhang, S. V. Dubonos, I. V. Grigorieva, and A. A. Firsov, Science **306**, 666 (2004).
[2] K. S. Novoselov, A. K. Geim, S. V. Morozov, D. Jiang, M. I. Katsnelson, I. V. Grigorieva, S. V. Dubonos and A. A. Firsov, Nature **438**, 197 (2005).
[3] Y. B. Zhang, Y. W. Tan, H. L. Stormer, and P. Kim, Nature **438**, 201 (2005).
[4] C. Berger, Z. M. Song, X. B. Li, X. S. Wu, N. Brown, C. Naud, D. Mayou, T. B. Li, J. Hass, A. N. Marchenkov, E. H. Conrad, P. N. First, and W. A. de Heer, Science **312**, 1191 (2006).
[5] T. Ohta, A. Bostwick, T. Seyller, K. Horn, and Eli Rotenberg, Science **313**, 951 (2006).
[6] S. Stankovich, D. A. Dikin, G. H. B. Dommett, K. M. Kohlhaas, E. J. Zimney, E. A. Stach, R. D. Piner, S. T. Nguyen, and R. S. Ruoff, Nature **442**, 282 (2006).
[7] K. Sasaki, S. Murakami, and R. Saito, J. Phys. Soc. Jpn. **75** (2006) 074713.
[8] K. Nakada, M. Fujita, G. Dresselhaus, and M. S. Dresselhaus, Phys. Rev. B **54**, 17954 (1996).
[9] M. I. Katsnelson, K. S. Novoselov, A. K. Geim, Nature Physics **2**, 620 (2006).
[10] O. Klein, Z. Phys. **53**, 157 (1927).
[11] R. Landauer, Philos. Mag. **21**, 863 (1970).
[12] J. Zhang, Q. W. Shi, and J. Yang, J. Chem Phys. **120**, 7733 (2004).
[13] S. Datta, Electronic Transport in Mesoscopic Systems (Cambridge University Press, New York, 1995).
[14] C. P. Chang, Y. C. Huang, C. L. Lu, J. H. Ho, T. S. Li, M. F. Lin, Carbon **44** 508 (2006).
[15] Katsunori Wakabayashi and Manfred Sigrist, Phys. Rev. Lett. **84**, 3390 (2000).